Study on Frequency Response of DBD Load

Pradeep[1] Dr. Radhe Shyam Jha 'Rajesh[2]

[1]Research Scholar, Singhania University, Rajasthan

[2]Principal, B.M. College of Technology & Management, Farukh Nagar (HR)

Abstract – The phase relation plot of the frequency response curves of DBD load as a function of angular frequency having the same C_d and C_g but different values of R is shown in figure 2. The results are shown for four values of R = (0, 10k, 100k and 2M ohm). From the phase plot of frequency response, it is evident that the equivalent reactance of the plasma reactor is negative indicating that the reactive part is due to capacitance. It implies that the DBD load is capacitive as seen from the secondary of high voltage transformer irrespective of frequency of operation and resistance R of the DBD load. However, as R is varied over a range from R=0 to 2M Ω a peak in phase curve is obtained, implying that there is a slight change in the capacitive nature of the load. Further, as R is increased the peak of this band shifts to a lower frequency. The DBD load has an equivalent circuit comprising a capacitor C_d of the dielectric barrier connected in series with a capacitor C_g of the gas gap, connected across the secondary winding of high voltage transformer and has a conducted path represented by R, when DBD discharge occurs

Key Words: Reactance, frequency, response, capacitive

---♦---

INTRODUCTION

US optical sources have been used in several areas including surface modification, material deposition/coating of metals, dielectrics (high and low dielectric constant materials), and semi conducting layers, hardening of paints, lacquers, and adhesives, for printing and lamination, in automotive and equipment engineering. The phase relation plot of the frequency response curves of DBD load as a function of angular frequency having the same C_d and C_g but different values of R is shown in figure 2. The results are shown for four values of R = (0, 10k, 100k and 2M ohm). From the phase plot of frequency response, it is evident that the equivalent reactance of the plasma reactor is negative indicating that the reactive part is due to capacitance. It implies that the DBD load is capacitive as seen from the secondary of high voltage transformer irrespective of frequency of operation and resistance R of the DBD load. However, as R is varied over a range from R=0 to 2M Ω a peak in phase curve is obtained, implying that there is a slight change in the capacitive nature of the load. Further, as R is increased the peak of this band shifts to a lower frequency. As it is now evident from the frequency response curves, wether the DBD is operated at low frequencies near about several kHz or at high frequency (near about rf) the DBD load always remains mainly capacitive.

REVIEW OF LITERATURE

UV radiation sources also have a potential impact on textile and polymer technology [Ersom *et al.,* 1992; Mehnert *et al.,* 2002] where they are used in surface treatment, e.g. surface modification of polymers, dry etching of polymers, synthesis of hydrophilic polymers to increase adhesion between metal and polymer, surface cleaning and surface etching including three-dimensional applications, and textile finishing. Furthermore, they are used in several photon initiated scientific and industrial applications [Lomaev *et al.*, 2006a] such as in the field of photo-chemistry, e.g. for photo-chlorination, photo-sulpho-oxidation, photo-nitrosylization, photo-oxidation, photo mineralization, actinometry etc., in photo-medicine, such as for the treatment of skin conditions, tanning etc., in photobiology for photo inactivation, photo regulation and photo destruction.

MATERIAL AND METHOD

The frequency characteristic estimation of DBD excimer gas discharge load is typically carried out using the equivalent circuit model shown in figure 1. The DBD load has an equivalent circuit comprising a capacitor C_d of the dielectric barrier connected in series with a capacitor C_g of the gas gap, connected across the secondary winding of high voltage transformer and has a conducted path represented by R, when DBD discharge occurs.

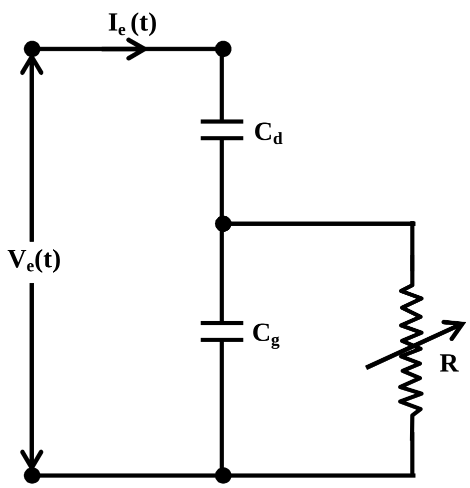

Figure 1 DBD excimer load equivalent circuit

From figure 1., the equivalent combination of $R \parallel \frac{1}{sC_g}$ can be written as:

$$Z_p(s) = \frac{R}{1+sRC_g}$$

The equivalent impedance of the circuit shown in figure 1 is given as:

$$Z_e(s) = \frac{1}{sC_d} + \frac{R}{1+sRC_g}$$

$$Z_e(s) = \frac{1+sR(C_d+C_g)}{sC_d(1+sRC_g)} = \frac{1+sR(C_d+C_g)}{(s^2RC_dC_g+sC_d)} \quad (1)$$

The frequency response of equation (1) is given as:

$$Z_e(j\omega) = \frac{1+j\omega R(C_d+C_g)}{j\omega C_d(1+j\omega RC_g)} \quad (5.2)$$

The magnitude $|Z_e(j\omega)|$ and phase angle $\varphi_z(j\omega)$ of equation (2) for $\omega > 0$ are:

$$|Z_e(j\omega)| = \frac{\sqrt{1+\omega^2R^2(C_d+C_g)^2}}{\sqrt{\omega^2C_d^2}\sqrt{1+\omega^2R^2C_g^2}} \quad (3)$$

$$\varphi_z(j\omega) = -90^\circ - \tan^{-1}(\omega RC_g) + \tan^{-1}(\omega R(C_d+C_g)) \quad (4)$$

The voltage gain of the DBD load is given as:

$$V(s) = \frac{V_g(s)}{V_e(s)} = \frac{sRC_d}{1+sR(C_d+C_g)} \quad 5)$$

The magnitude $|V(j\omega)|$ and phase angle $\varphi_v(j\omega)$ of equation (5) for $\omega > 0$ are:

$$|V(j\omega)| = \frac{\sqrt{\omega^2R^2C_d^2}}{\sqrt{1+\omega^2R^2(C_d+C_g)^2}} \quad (6)$$

$$\varphi_v(j\omega) = 90^\circ - \tan^{-1}(\omega R(C_d+C_g)) \quad (7)$$

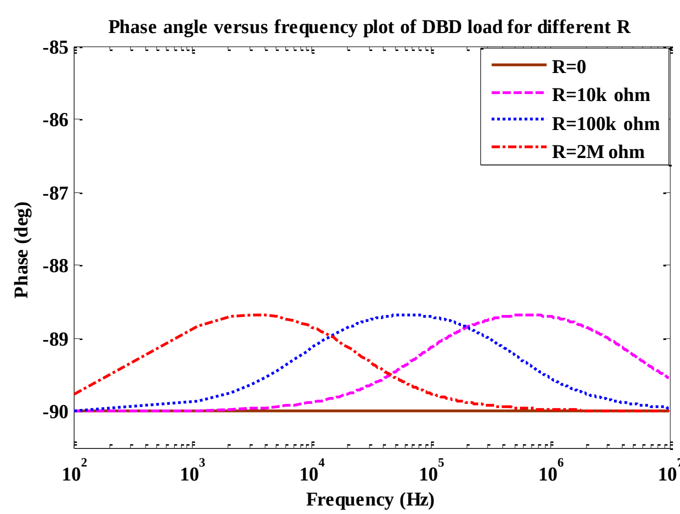

Figure 2 Phase angle versus frequency plot of DBD load for different R

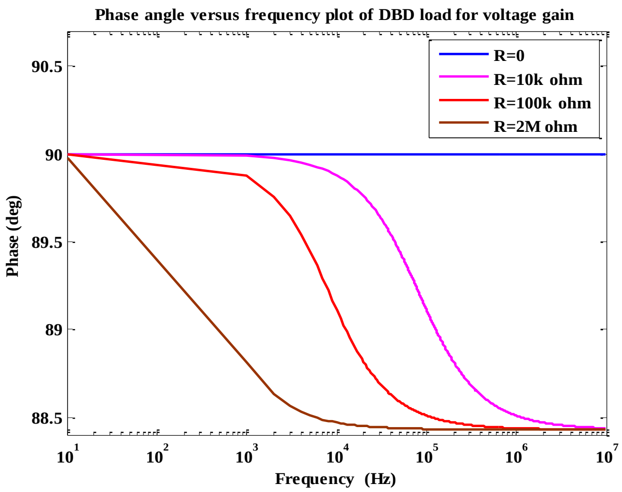

Figure 3 Phase angle versus frequency plot of DBD for voltage gain

Therefore, in order to drive the DBD over a wide frequency range, it is necessary to achieve impedance matching of the DBD load. The phase curve of frequency response of voltage gain is depicted in figure 3.

Simplified Model of DBD

In order to carry out the high frequency modeling of DBD load, the non-linear model of DBD discussed earlier is transformed into a simplified linear model. This has also beeen done for a [Haverkamp *et al*., 2002; Alonso *et al.,* 2003; Alonso *et al.,* 2004] non-linear model of silent discharge ozonator which was transformed into a simplified linear model, which is quite simple and is useful for the design of several technological applications of DBD at higher frequency. The simplified model follows from the previous model that the two capacitors C_d and C_g can be integrated into a single capacitor C_e and the plasma be modeled as linear resistor. This simplified model consists of equivalent capacitance C_e and equivalent resistance R_e in parallel. In fact, more complicated plasma circuit models present in the literature [Wang *et al.,* 1999; Koudriavtsev *et al.,* 2000; Francke *et al.*, 2003] can also be actually transformed into the simplified model by circuit analysis technique as shown in figure 5.4. The equivalent capacitance of plasma reactor C_e and equivalent resistance R_e parameters of this linear model can be easily obtained from the Lissajous figures of voltage-current and voltage-charge characteristic of the DBD reactor.

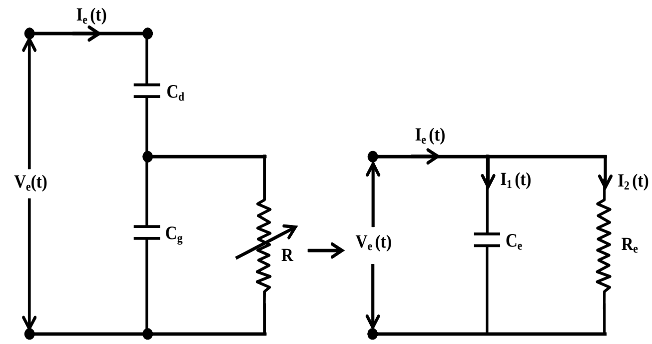

Figure 4 Transformation of nonlinear model

From figure 4, according to Kirchhoff's current law, the total external current, $I_e(t)$, is simply given as sum of $I_1(t)$ and $I_2(t)$, as follows:

$$I_e(t) = I_1(t) + I_2(t)$$

Assuming the typical voltage applied to drive DBD reactor at high frequency to be a pure sinusoidal wave of amplitude V_s angular frequency ω is given as:

$$V_e(t) = V_s \sin \omega t$$

The total current $I_e(t)$, in simplified electrical model can be written as:

$$I_e(t) = C_e \frac{dV_e(t)}{dt} + \frac{V_e(t)}{R_e} \quad (5.8)$$

where $I_1(t)$ and $I_2(t)$ are the current flowing through equivalent C_e and R_e respectively.

$$I_e(t) = \frac{V_s}{X_e} \cos \omega t + \frac{V_s}{R_e} \sin \omega t \quad (5.9)$$

$$I_e(t) = \frac{V_s}{Z_e} \sin(\omega t + \varphi_e)$$

where $X_e = \frac{1}{\omega C_e}$, $Z_e = \sqrt{(R_e^2 + X_e^2)}$ and

$$\varphi_e = \tan^{-1}\frac{X_e}{R_e}$$

From equation (5.8) and (5.9), the time variable can be cancelled and equation (5.9) can be rewritten as:

$$I_e(t) = \frac{V_e(t)}{R_e} + \frac{1}{X_e}\sqrt{\left(V_s^2 - V_e^2(t)\right)} \qquad (5.10)$$

On putting $V_e(t) = 0$ in equation (5.10), the corresponding value of current I_0 can be calculated as follows:

$$I_0 = \frac{V_s}{X_e}$$

Corresponding to equation (5.10), Lissajous figure can be obtained, therefore by measuring the value of I_0 from the Lissajous figure of the discharge cell, the equivalent parallel capacitance can be calculated using the expression:

$$C_e = \frac{I_0}{\omega V_s} = \frac{I_0}{2\pi f V_s} \qquad (5.11)$$

Also, from equation (5.8), the relationship between current and charge is given as:

$$I_e(t) = \frac{dq}{dt}$$

On integrating equation (5.8), charge in the DBD cell is given as:

$$q = C_e V_e(t) + \frac{1}{R_e}\int V_e(t)dt \qquad (5.12)$$

For the typical case of a sinusoidal supply voltage across the excimer tube given by (5.12), the charge in the DBD cell is given as:

$$q = C_e V_s \sin\omega t - C_R V_s \cos\omega t = C_E V_s \sin(\omega t - \varphi) \qquad (5.13)$$

where, $C_R = \frac{1}{\omega R_e}$, $C_E = \sqrt{\left(C_e^2 + C_R^2\right)}$, and

$$\varphi = \tan^{-1}\frac{C_R}{C_e}$$

From equation (5.13) the time varying variables can be cancelled and correspondingly charge q is given as follows:

$$q = C_e V_e(t) + C_R\sqrt{\left(V_s^2 - V_e^2(t)\right)} \qquad (5.14)$$

On putting $V_e(t) = 0$ in the equation (5.14), correspondingly q_0 is given as:

$$q_0 = C_R V_s \qquad (5.15)$$

The charge q_0 corresponding to equation (5.15) is obtained from the Q-V Lissajous diagram of DBD. Thus, the equivalent parallel resistance R_e of excimer tube is given as follows:

$$R_e = \frac{V_s}{\omega q_0} = \frac{V_s}{2\pi f q_0} \qquad (5.16)$$

By solving the system of equations given by equations (5.8) to (5.16), the equivalent network parameters C_e and R_e of the simplified model can be obtained. The equivalent impedance of the simplified linear model shown in figure 5.4 is given as:

$$Z_s(s) = \frac{R_e}{1 + sR_eC_e} \qquad (5.17)$$

The frequency response function of equation (5.17) is given as:

$$Z_s(j\omega) = \frac{R_e}{1 + j\omega R_e C_e}$$

The magnitude $|Z_e(j\omega)|$ and phase angle $\varphi\ (j\omega)$, for $\omega > 0$ are:

$$|Z_s(j\omega)| = \frac{R_e}{\sqrt{1 + \omega^2 R_e^2 C_e^2}} \qquad (5.18)$$

$$\varphi(j\omega) = -\tan^{-1}\omega R_e C_e \qquad (5.19)$$

Conclusion

As ω is varied from minimum ($\omega \to 0$) to maximum ($\omega \to \infty$), the corresponding variation in phase angle occurs from 0 to 90°, it implies that the DBD load is capacitive at higher frequency and needs impedance matching to operate at higher frequency. It is mathematically much simpler to set up a relation between applied voltages driving the DBD cell and equivalent circuit parameters of this linear model. The simplified model avoids non-linear condition of the discharge and is therefore intended to serve the purpose of estimation of load matching conditions of DBD load. Although this simplified model does not explain the physical working of the discharge reactor, but it is highly advantageous in several design objectives such as in impedance matching of the DBD reactor.

REFERENCES

1. Alonso J M, Valdes M, Calleja A J, Ribas J and Losda J, High frequency testing and modelling of silent discharge ozone generators, Ozone Science and Engineering, vol. 25, pp. 363-376, 2003.

2. Babayan S E, Jeong J Y, Schutze A, Tu V J, Selwyn G S and Hicks R F, Deposition of silicon dioxide films with a non–equilibrium atmospheric pressure plasma jet, Plasma Sources Sci. Technol., vol. 10, pp. 573-578, 2001.

3. Babu K M and Shankar G, Application of plasma in textile industry, Asian Textile Journal, pp. 63-67, May 2005.

4. Basting D, Pippert K and Stamm U, History and future prospects of excimer laser technology, Proc. 2nd International Symposium on Laser Precision Micro fabrication, pp. 14-22, 2002.

5. Becker K H, Kogelschatz U, Barker R J and Schoenbach K H, Non-equilibrium air plasma at atmospheric pressure, IOP, 2004.

6. Becker K H, Schoenbach K H and Eden J G, Microplasmas and applications, J. Phys. D: Appl. Phys., vol. 39, pp. R55-R70, 2006.

7. Bergonzo P and Boyd I W, Low-pressure photo deposition of silicon nitride films using a xenon excimer lamp, Appl.Phys. Lett. vol. 63, no.13, pp. 1757-1759, 1993.

8. Bergonzo P, Patel P, Boyd I W and Kogelschatz U, Development of a novel large area excimer lamp for direct photo deposition of thin films, Appl. Surf. Sci., vol. 45, pp. 424-429, 1992.

9. Bhoj A N and Kushner M J, Plasma polymer interactions in a dielectric barrier discharge, IEEE Trans. Plasma Sci., vol. 33, no.2, pp. 250-251, 2005.

10. Bhosle S, Zissis G, Damelincourt J J and Dawson F P, Calculation of the impedance of an axisymmetric DBD lamp for power supply design purposes, Industry Applications Conferences IEEE , vol. 3, pp. 1667-70, 2004.

11. Bhosle S, Zissis G, Damelincourt J J, Capdevila A, Gupta K, Dawson F P and Tarasenko

12. Bogaerts A, Neyts E, Gijbels R and Mullen J V D, Gas discharge plasmas and their applications. Spectrochimica Acta Part B, vol. 57, pp. 609-658, 2002.

13. Bogaerts A, The glow discharge: an exciting plasma, J. Anal. At. Spectrom., vol. 14, pp. 1375-1384, 1999.

14. Boichenko A M, Yakovlenko and V F Tarasenko, Electron beam excited Xe excillamp optimal characteristic, Laser and Particle Beams, vol. 18, pp. 655-660, 2000.

15. Bonnizzoni G and Vassallo E, Plasma physics and technology; industrial applications, Vacuum, vol. 64, pp. 327-336, 2002.

16. Boulos M I, Fauchais P and Pfender E, Thermal plasma: Fundamental and applications, vol. 1, Plenum Press, New York, 1994.

17. Boulos M I, New frontiers in thermal plasma processing, Pure Appl. Chem., vol. 68, pp. 1007-1010, 1996.

18. Boulos M I, Thermal plasma processing, IEEE Trans. Plasma Sci., vol. 19, pp. 1078-1089, 1991.

19. Boyd I W and Zhang J Y, Photo induced growth of dielectrics with excimer lamp, Appl. Surf. Sci., vol. 54, pp. 1413-1431, 2001.

20. Chang J S, Lawless P A and Yamamoto T, Corona discharge processes, IEEE Trans. Plasma Sci., vol. 19, pp. 1152-1166, 1991.

21. Chen F, Introduction to plasma physics and controlled fusion, Plenum Press, New York, 1984.

22. Chen Z, Impedance matching for one atmospheric uniform glow discharge plasma (OAUGDP) reactors, IEEE

Trans. Plasma Sci., vol. 30, no.5, pp. 1922-1929, 2000.

23. Chirokov A, Gutsol A and Fridman A, Atmospheric pressure plasma of dielectric barrier discharges, Pure Appl. Chem., vol. 77, pp. 487-495, 2005.

24. Conrads H and Schmidt M, Plasma generation and plasma sources, Plasma Sources Sci. Technol., vol. 9, pp. 441-454, 2000.

25. Dakin J T, Nonequilibrium lighting plasmas, IEEE Trans. Plasma Sci., vol. 19, pp. 991-1002, 1993.

26. Eliasson B and Kogelschatz U, Non-equilibrium volume plasma chemical processing, IEEE Trans Plasma Sci, vol. 19, pp. 1063-1077, 1991.

27. Eliasson B, Egli W and Kogelschatz U, Modelling of dielectric barrier chemistry, Pure Appl. Chem., vol. 66, no.6, pp. 1275-1286, 1994.

28. Eliasson B, Hirth M and Kogelschatz U, Ozone synthesis from oxygen in dielectric barrier discharges, J. Phys. D: Appl. Phy., vol. 20, pp. 1421-1437, 1987.

29. Eliasson B and Kogelschatz U, UV excimer radiation from dielectric-barrier discharges, Appl. Phys. B: Laser & Optics, vol. 46, pp. 299-303, 1988a.

30. Eliasson B and Kogelschatz U and Stein H J, New trends in high intensity UV radiations, EPA Newsletter, vol. 32, pp. 29-40, 1988b.

31. Falkenstein Z and Coogan J J, The development of silent discharge driven $XeBr^*$ excimer UV source, J. Phys. D: Appl. Phys., vol. 30, pp. 2704-2710 1997.

32. Fauchais P and Vardelle A, Thermal plasmas, IEEE Trans. Plasma Sci., vol. 25 pp. 1258-1270, 1997.

33. Fuentes A A F, Eguiluz R P, Callejas R L, Cabrera A M, Barocio S R, Cabrera O G, Read B J S, Sotelo J P, Modeling and simulation of a DBD plasma discharge supplied by a multicell inverter, Proc. 25th IASTED International Conference Modeling, Identification and Control, Feburary 6-8, Lanzarote, Canary Island, Spain, pp. 249-254, 2006a.

34. Fuentes A A F, Eguiluz R P, Callejas R L, Cabrera A M, Barocio S R, Cabrera O G, Read B J S and Sotelo J P, A multicell converter model of DBD plasma discharge, AIP Conf. Proc., Plasma and Fusion Science, vol. 875, December 4, pp. 188-191, 2006b.

35. Gupta B, Plasma processing: Some basic considerations. Plasma Physics, Wiely Eastern Limited, pp. 170-211,1992.

36. Habachi A E and Schoenbach K H, Generation of intense excimer radiation from high-pressure hollow cathode discharges, Appl. Phys. Lett., vol 73, pp. 885-887, 1998.

37. Haverkamp R G, Miller B B and Free K W, Ozone production in a high frequency

38. Ivanov V V, Kolpovsokii K S, Mankelevich Y U, Rakhimov A T, Rulev G B and Senko V B, Experimental and theoretical study of the efficiency of an excimer lamp by a pulsed distributed discharge in xenon, Laser Phys., vol. 6, pp. 654-659, 1996.

39. Jeong J Y, Babayan S E, Tu V J, Park J, Henins I , Hicks R F and Selwyn G S, Etching materials with an atmospheric pressure plasmas jet, Plasma Sources Sci. Technol., vol. 7, pp. 282-285, 1998.

40. John P I, Plasma science and creation of wealth, Tata McGraw Hill, India 2005.

41. Kogelschatz U, Atmospheric-pressure plasma technology, Plasma Phys. Control. Fusion, vol. 46, pp. B63-B75, 2004.

42. Kogelschatz U, Dielectric-barrier discharges: Their history, discharge physics, and industrial applications, Plasma Chem. and Plasma Process., vol. 23, no.1, pp. 1-46, 2003.

43. Kogelschatz U, Eliasson B and Egli W, Dielectric barrier discharges principal and applications, ICPIG XXIII, July 17-22, Toulouse, France, 1997.

44. Kogelschatz U, Eliasson B and Egli W, From ozone generators to flat television screens: history and future potential of dielectric barrier discharges, Pure Appl. Chem., vol. 71, no.10, pp. 1819-1828, 1999.

45. Kurunczi P, Shah H and Becker K, Hydrogen Lyman-a and Lyman-a emissions from high-pressure microhollow cathode discharges in Ne-H_2 mixtures, J. Phys. B: At. Mol. Opt. Phys. vol. 32, pp. L651-L658, 1999.

46. Lakoba S and Yakovlenko S I, Active media of exciplex lasers, Sov. J. Quantum Electron., vol. 10, pp. 389-410, 1980.

47. Lieberman M A and Lichtenberg A J, Principles of plasma discharges and material processing, Wiley, New York, 1994.

48. Lister G G, Lawler J E, Lapatovich W P and

Godyak V A, The physics of discharge lamps, Review of Modern Phys., vol. 76, pp. 541-598, 2004.

49. Lomaev M I, Sosnin E A and Tarasenko V F, Capacitive and barrier discharge excilamps and their applications, Instruments & Experimental Technique, vol. 49, no.5, pp. 595-646, 2006a.

50. Lomaev M I, Sosnin E A and Tarasenko V F, Applications of capacitive and barrier discharge excillamps in photoscience, Journal of Photochemistry and Photobiology C: Photochemistry Reviews, vol. 7, no.4, pp. 145-163, 2006b.

51. Massines F and Gouda G, A comparison of polypropylen-surface treatment by filamentary, homogeneous and glow discharges in helium at atmospheric pressure, J. Phys. D: Appl. Phys., vol. 31, pp. 3411–3420, 1998.

52. Massines F, Gadri R B, Decomps P, Rabehi A, Ségur P and Mayoux C, Atmospheric pressure dielectric controlled glow discharges: Diagnostics and modeling, Proc. 22rd ICPIG, vol. 363, Hoboken, NJ, pp. 306–315, 1996.

53. Massines F, Mayoux C, Messaoudi R, Rabehi A and Segur P, Experimental study of an atmospheric pressure glow discharge application to polymers surface treatment, Proc. 10th Ind. Conf. Gas Discharges and Their Applications, Swansea, U.K, vol. 2, pp. 730–733, 1992.

54. Montie T C, Kelly-Wintenberg K and Roth J R, An overview of research using a one atmosphere uniform glow discharge plasma (OAUGDP) for sterilization of surfaces and materials, IEEE Trans. Plasma Sci., vol. 28, pp. 41–50, 2000.

55. Morimoto Y, Sumitomo T, Yoshioka M and Takemura T, Recent progress on UV lamps for industries, Industry Applications Conferences IEEE, vol. 2, pp. 1008–1015, 2004.